IOP PUBLISHING PHYSICS IN MEDICINE AND BIOLOGY

Phys. Med. Biol. **54** (2009) 5949–5963 doi:10.1088/0031-9155/54/19/019

# *In vivo* electrical conductivity measurements during and after tumor electroporation: conductivity changes reflect the treatment outcome

**Antoni Ivorra**[1,6], **Bassim Al-Sakere**[2,3], **Boris Rubinsky**[4,5] **and Lluis M Mir**[2,3]

[1] Departments of Mechanical Engineering and Bioengineering, University of California at Berkeley, Berkeley, CA 94720, USA
[2] UMR 8121 CNRS-Institut Gustave-Roussy, Villejuif 94805, France
[3] Univ Paris-Sud, UMR 8121, France
[4] Department of Bioengineering, Department of Mechanical Engineering and Graduate Program in Biophysics, University of California at Berkeley, Berkeley, CA 94720, USA
[5] Center for Bioengineering in the Service of Humanity and Society, School of Computer Science and Engineering, Hebrew University of Jerusalem, Givat Ram, Jerusalem 91904, Israel

E-mail: antoni.ivorra@gmail.com

Received 5 June 2009, in final form 19 August 2009
Published 17 September 2009
Online at stacks.iop.org/PMB/54/5949

**Abstract**

Electroporation is the phenomenon in which cell membrane permeability is increased by exposing the cell to short high-electric-field pulses. Reversible electroporation treatments are used *in vivo* for gene therapy and drug therapy while irreversible electroporation is used for tissue ablation. Tissue conductivity changes induced by electroporation could provide real-time feedback of the treatment outcome. Here we describe the results from a study in which fibrosarcomas ($n = 39$) inoculated in mice were treated according to different electroporation protocols, some of them known to cause irreversible damage. Conductivity was measured before, within the pulses, in between the pulses and for up to 30 min after treatment. Conductivity increased pulse after pulse. Depending on the applied electroporation protocol, the conductivity increase after treatment ranged from 10% to 180%. The most significant conclusion from this study is the fact that post-treatment conductivity seems to be correlated with treatment outcome in terms of reversibility.

(Some figures in this article are in colour only in the electronic version)

## 1. Introduction

Electroporation, or electropermeabilization, is the phenomenon in which cell membrane permeability to ions and macromolecules is increased by exposing the cell to short

[6] Author to whom any correspondence should be addressed.

  

(microseconds to milliseconds) high-electric-field pulses (Neumann *et al* 1982). The permeabilization can be temporary (reversible electroporation) or permanent (irreversible electroporation) as a function of the electric field magnitude and duration, period and number of the pulses. Both reversible and irreversible electroporation have important applications in biotechnology and medicine (Mir 2001). Reversible electroporation is now commonly used with microorganisms and cells in culture for transfection or for introduction or removal of macromolecules from individual cells. Irreversible electroporation is used for sterilization of liquid media from microorganisms. During the last two decades, reversible electroporation has started to be used in living tissues for *in vivo* gene therapy (electrogenetherapy) (Jaroszeski *et al* 2000, Dean 2005) and to enhance the penetration of anti-cancer drugs into undesirable cells (electrochemotherapy, ECT) (Gothelf *et al* 2003). Recently, irreversible electroporation (IRE) has also found a use in tissues as a minimally invasive surgical procedure to ablate undesirable tissue without the use of adjuvant drugs (Davalos *et al* 2005, Miller *et al* 2005, Edd *et al* 2006, Rubinsky *et al* 2007).

*In vivo* electroporation depends on too many factors to be reliably applied in an open-loop procedure (Cegovnik and Novaković 2004, Pucihar *et al* 2001). Real-time feedback from the outcome of the applied pulse or pulses is a requirement if it is desired to control electroporation by means of the magnitude, number or duration of the pulses (Cukjati *et al* 2007, Glahder *et al* 2005).

A set of possible methods for assessing the effects of electroporation could be based on measurements of the passive electrical properties of the electroporation-affected cells or tissues (Ivorra and Rubinsky 2007, Pliquett *et al* 2004, Grafström *et al* 2006, Cima and Mir 2004, Pavlin *et al* 2005, Kinosita and Tsong 1979). As a matter of fact, electroporation phenomenon was first described in electrical terms (Stämpfli 1957). Measuring changes in electrical properties of cells has been proposed for determining the effectiveness of electroporation protocols in individual cells (Huang and Rubinsky 1999) and in cell cultures (Glahder *et al* 2005, Pavlin *et al* 2005). Similarly, changes in electrical properties were proposed for detecting electroporation in tissues (Dev *et al* 2003), including the creation of images of the electroporated tissue volumes by means of electrical impedance tomography (Davalos *et al* 2002).

The present study is part of a comprehensive effort to fully characterize the changes in electrical properties of tissues with reversible and irreversible electroporation. It is preceded by similar but simpler studies in rat liver (Ivorra and Rubinsky 2007) and in rat skeletal muscle (Ivorra *et al* 2007).

In another previous study (Al-Sakere *et al* 2007), the efficiency of different electroporation protocols for ablating tumors by IRE was assessed. Here we have employed some of those protocols and we have compared the results in terms of impedance properties and of tissue damage.

## 2. Methods

### *2.1. Tumor cell culture and tumor production*

Cells from a LPB cell line, a methylcholanthrene-induced C57 Bl/6 mouse sarcoma cell line (Belehradek *et al* 1972), were cultured using standard procedures in a minimum essential medium (Gibco BRL, Cergy-Pontoise, France) supplemented with 100 U $ml^{-1}$ penicillin, 100 mg $ml^{-1}$ streptomycin (Sarbach, France) and 8% fetal calf serum (Gibco). C57 Bl/6 female mice, 6–8 weeks old, were inoculated subcutaneously in the left flank with

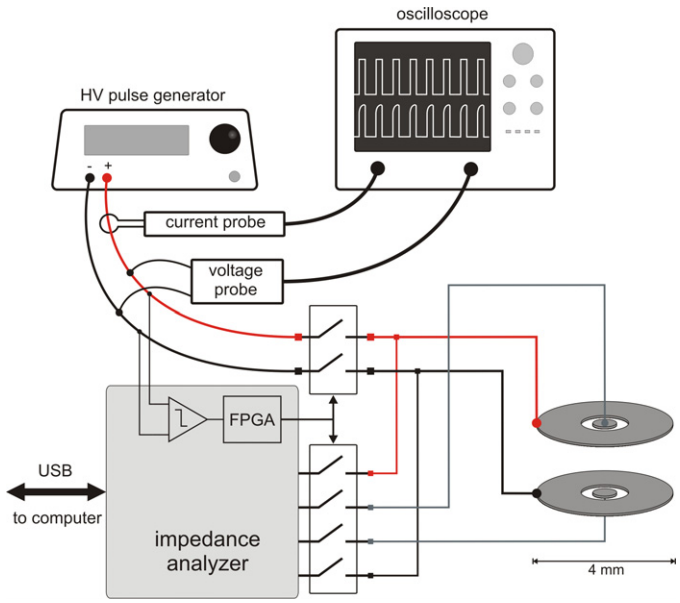


**Figure 1.** Architecture of the measurement system. The 'in-pulse' conductance is recorded by the oscilloscope during the electroporation pulses whereas AC impedance is measured afterward.

$1 \times 10^6$ cells, producing in 9 days tumors 4–5 mm in diameter. Animals were housed and handled according to the recommended guidelines (UKCCCR 1998).

### *2.2. Surgical process and tumor treatment*

At the start of the procedure, mice were anesthetized with volatile anesthetic (Isoflurane (Belamont, Neuilly, France) with the vaporizer at 4% for anesthesia induction and 1.5% for anesthesia maintenance. An incision was performed on the skin near the tumor and the skin flap containing the tumor was lifted, taking particular care to avoid cutting the main blood vessels nourishing the tumor. The plate electrodes were placed in direct contact with both sides of the cutaneous tumor, with the tumor sandwiched between the parallel plates. The distance between the electrodes ranged from 1.5 to 3 mm and was adjusted to tumor size. The spacing between the electrodes was measured and the information was used to set the voltage delivered by the pulse generator so that the electric field magnitude matched the value specified by the protocol (see section 2.4). The square-wave electric pulses (EP) were generated by an electroporation power supply (Cliniporator$^{TM}$, Igea, Carpi, Italy) able to apply high-voltage pulses with a repetition frequency ranging from 1 Hz to 5 kHz. To obtain a pulse application frequency of 0.03 Hz (see protocol 3 in section 2.4), single pulses were manually delivered by the operator every 33 s.

### *2.3. Measurement system*

Measurement methods were the same that those employed in Ivorra and Rubinsky (2007). Here we briefly summarize them and indicate some differences.

The general architecture of the measurement system is shown in figure 1. The electroporation voltage pulses were applied to the sample through a pair of large annular

electrodes (here the outer diameter is 4 mm instead of 10 mm (Ivorra and Rubinsky 2007)), represented at the bottom right corner of figure 1. For each experiment the voltage value ($V$) was selected so that the ratio $V/d$, where $d$ was the distance between the electrodes, was equal to the desired electric field magnitude of the protocol (see section 2.4).

Passive electrical properties of the tissue were measured during and after the application of the electroporation pulse thanks to an automated switching mechanism. After the electroporation pulse, the impedance of the tissue between the electrodes was measured using the four-electrode method in which the electroporation electrodes (outer diameter = 4 mm, inner diameter = 1 mm) were used as current injection electrodes (100 $\mu$A) and a pair of smaller inner electrodes (diameter = 0.7 mm) were used to measure the induced voltage difference across the tissue sample. Recording of current and voltage during the electroporation pulse application was performed with special oscilloscope probes (current probe AP015 and high-voltage probe ADP305 from LeCroy Corp.). From these two signals we computed the 'in-pulse' conductance.

The system was configured to measure in a bi-frequency mode (1 kHz and 15.5 kHz) between the pulses and up to 500 ms after the end of last pulse at a rate of 500 samples per second. After this time point, frequency scans (11 frequencies from 1 kHz to 400 kHz at a rate of 20 scans per second) were recorded for 30 min. Nevertheless, as it will be noted in section 3.1, we discovered that the multi-frequency analysis was not interesting in the experimental study presented here and we focused our analysis only on data acquired at 1 kHz. Therefore, the system was in fact used as a single frequency (1 kHz) impedance meter.

Conductivity values were obtained by scaling conductances according to the cell factors as computed by means of Finite Element Method tools as shown in Ivorra and Rubinsky (2007). The size of tumors was not uniform and resulted in electrode plate separations ranging from 1.5 to 3 mm.

### *2.4. Electroporation protocols*

A total number of 39 LPB fibrosarcomas inoculated in mice were treated according to one of the following electroporation protocols:

- *Protocol 1*: 8 pulses of 100 $\mu$s at a frequency of 10 Hz, electric field magnitude from 450 V cm$^{-1}$ to 3500 V cm$^{-1}$; five groups (450, 1000, 1500, 2500 and 3500 V cm$^{-1}$) of five tumors.
- *Protocol 2*: 8 pulses of 100 $\mu$s at a frequency of 1 Hz, electric field magnitude = 2500 V cm$^{-1}$; single group of five tumors.
- *Protocol 3*: 8 pulses of 1000 $\mu$s at a frequency of approximately 0.03 Hz, electric field magnitude = 2500 V cm$^{-1}$; single group of four tumors.
- *Protocol 4*: 80 pulses (delivered in four series of 20 pulses separated by approximately 5 s) of 100 $\mu$s at a frequency of 1 Hz, electric field magnitude = 2500 V cm$^{-1}$; single group of five tumors.

DC conductance was measured during the pulses ('in-pulse' conductance) and AC impedance was recorded in the inter-pulse intervals and for 30 min after the electroporation sequence.

## 3. Results and discussion

### *3.1. Tumor impedance before treatment*

In Ivorra and Rubinsky (2007), we employed Cole model in order to parameterize the impedance spectrogram of rat liver. Here we have obtained some impedance spectrograms

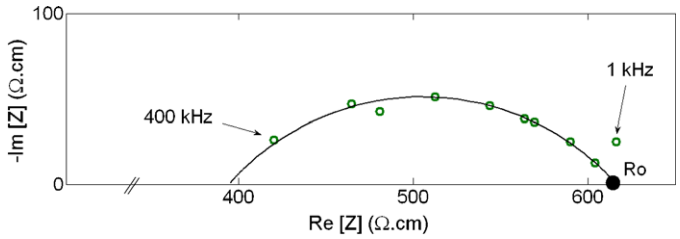


**Figure 2.** Example of impedance locus (imaginary part of impedance, Im [*Z*], versus real part of impedance, Re [*Z*]) before electroporation. Circles denote actual data and the continuous line depicts the corresponding Cole model. Measured impedance values are scaled according to the probe cell constant in order to provide impedivity values.

somehow suitable for Cole modeling (see figure 2); however, in most cases tumors produced responses not compatible with any sort of simplified impedance spectrum model for living tissues. This phenomenon was observed before in human breast tumors (Jossinet and Schmitt 1999) and it may be related to the fact that tumors are highly heterogeneous and disordered cell structures. For the sake of simplicity and reliability, here we decided not to use Cole modeling. In fact, here we only report and analyze the conductivity values. More precisely: all post-pulse conductivity values that we provide in this paper are in fact admittivity magnitude values at 1 kHz.

We considered impedance measurements before electroporation from 15 out of 25 tumors in protocol 1 in order to compute the original conductivity (mean $\sigma_0$). Small tumors (distance between plates <2 mm) were rejected for such purpose because they provided erratic values. The resulting value is 1.35 ± 0.19 mS cm$^{-1}$ (mean ± standard deviation). This value represents the admittivity magnitude at 1 kHz that we estimate to be close (error <5%) to the DC conductivity value. Such a statement is based on repetitive observation that the $R_0$ value (inverse of the DC conductivity), in those cases where Cole modeling was possible, was almost identical to the magnitude of the impedance at 1 kHz (e.g. see figure 2).

In all the following experiments we have rejected data that came from experiments in which the separation distance between plates was less than 1.6 mm or that came from experiments in which the initial conductivity was not within a ±40% tolerance range of the mean value given here (1.35 mS cm$^{-1}$).

### *3.2. Conductivity between and after the pulses*

A simplistic electrical model of the biological cell can be used to qualitatively understand the effects of electroporation on the tissue passive electrical properties. In such a model, a resistance representing the extracellular medium is in parallel with a capacitance accounting for the cell membrane in series with a resistance representing the intracellular medium. When electropermeabilization is achieved, then the membrane capacitance is partially shunted by a membrane resistance. Afterward, resealing of the membrane causes the shunting resistance to increase and the impedance tends to return to its original values.

And indeed the experimental results seem to fit that model: each pulse causes an immediate increase in conductivity that is followed by a slow tendency toward the original conductivity value (figures 3 and 4). Such 'recovery' tendency becomes slower with time. At first glance, the response could be modeled by a time-exponential function of the type

$$\sigma(t) = A + B \cdot \mathrm{e}^{\frac{-(t-t_0)}{\tau}}, \tag{1}$$

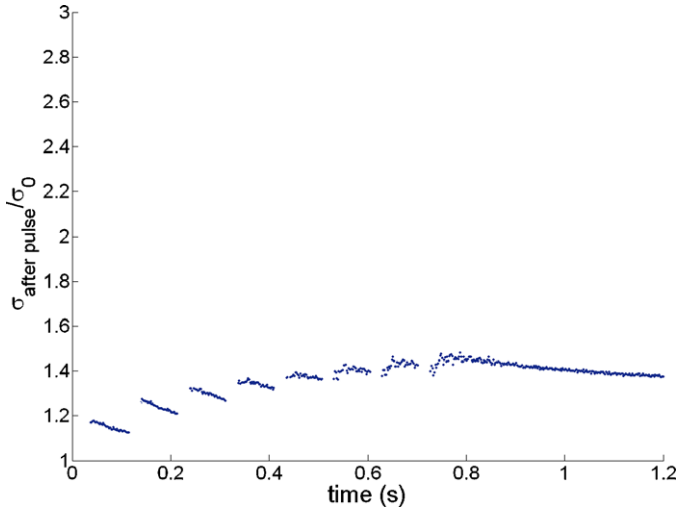


**Figure 3.** Relative conductivity between pulses and for a short period after pulses from an experiment belonging to protocol 1 (eight pulses of 100 $\mu$s at 10 Hz) at 2500 V cm$^{-1}$. $\sigma_0$ denotes the original conductivity of the sample, that is, before any pulse has been applied.

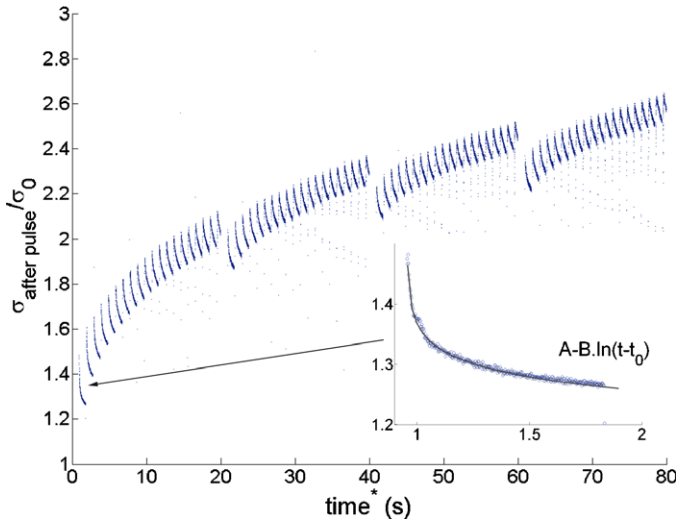


**Figure 4.** Relative conductivity between pulses from an experiment belonging to protocol 4 (80 2500 V cm$^{-1}$ pulses of 100 $\mu$s at 1 Hz, delivered in four series of 20 pulses separated by approximately 5 s). The inset shows a magnification of the response after the first pulse.

where $\sigma$ is the conductivity, $t - t_0$ is the time after the end of the pulse and $\tau$ is the 'time constant', a scalar, and A and B are also scalars. That would be in agreement with the model presented in DeBruin and Krassowska (1999) in which the decay in the number of pores after the pulse follows an exponential function. However, for the time range considered here (from 10 ms to 1 s after pulse ends), we have noted that responses can be much better approximated by time-logarithm functions of the type (see figure 4)

$$\sigma(t) = A - B \cdot \ln(t - t_0). \tag{2}$$

This sort of time-logarithmic conductivity decay can be also observed in results from other electroporation studies (Ghosh *et al* 1993) although, to the best of our knowledge, it has never been noted. In other physical phenomena in which time-logarithmic relaxations are observed, such a behavior is attributed to a distribution of relaxation constants (Prozorov and Prozorov 2004). Here it seems plausible that due to the heterogeneity of tissues, and in particular of tumors, the leaky sites induced by electroporation pulses could manifest a wide range of resealing time constants. Therefore, this result does not necessarily contradict the exponential decay model in DeBruin and Krassowska (1999).

An obvious observation in figures 3 and 4 is the accumulative effect of the pulses. That is, each pulse increases the conductivity of the tumor. However, it is also clearly observable that the step in conductivity is smaller pulse after pulse. This is quite reasonable when it is taken into account that (1) electroporation phenomenon depends on the transmembrane voltage and (2) the transmembrane voltage induced by an external electric field depends on the conductivity of the membrane. In other words, as the membrane conductance increases due to permeabilization, it is more difficult to achieve the required transmembrane voltage for further permeabilization. On the other hand, it is also noticeable, particularly in figure 3, that the decay in conductivity slows down pulse after pulse. Hence, pulse repetitions not only increase permeabilization but also make it more stable. This can be related to the models in which long, or multiple, pores increase the radius of previously created pores, thus making them more stable (DeBruin and Krassowska 1999), or to models in which the multiple pores increase the probability for the formation of the so called long-lived pores (Pavlin and Miklavcic 2008).

A key objective of the study presented here was to assess whether impedance changes induced by electroporation are related to treatment outcome so that this sort of measurements could be employed in a closed looped fashion for electroporation control. In this sense, it is understandable that the instantaneous conductance increase after electroporation treatment could be valuable as it reflects the increase in membrane permeability. Since conductance can decrease quite fast after the electroporation pulse (figures 3 and 4), it is necessary to define a precise time point at which the 'instantaneous' conductance increase is calculated. We have chosen to analyze measurements 50 ms after the end of the last pulse. This time point is both sufficiently large to allow relay switching and circuitry settling after the end of the high-voltage pulse and sufficiently small to allow measurement between electroporation pulses at 10 Hz (i.e. interval between pulses = 100 ms). Figure 5 shows relative conductivity after treatment (ratio between conductance 50 ms after treatment and conductance before treatment). These results show some interesting clear features: (1) protocols 3 and 4 at 2500 V cm$^{-1}$ produce significantly higher conductivities than protocol 1, even at 3500 V cm$^{-1}$; (2) the conductivity after protocol 1 seems to be quite constant up to 1500 V cm$^{-1}$; (3) the average conductivity increase for protocol 2 is similar to that for protocol 1 at 2500 V cm$^{-1}$.

In a previous study (Al-Sakere *et al* 2007), some of the electroporation protocols employed here were tested in order to determine whether they resulted in reversible or irreversible electroporation. The parameters set for protocol 1 (eight pulses of 100 $\mu$s at 10 Hz) correspond to the parameters employed to perform electrochemotherapy of superficial tumors with cytotoxic drugs (Gothelf *et al* 2003). However, without those cytotoxic drugs, this electroporation protocol did not produce significant changes in tumor evolution for electric field magnitudes below 2000 V cm$^{-1}$. In the absence of those drugs, at 3300 V cm$^{-1}$ (actually not reported in Al-Sakere *et al* (2007)), it was noted that tumor growth was significantly slowed down but complete tumor regression was not achieved, indicating partial achievement of irreversible electroporation. On the other hand, also in the absence of cytotoxic drugs, protocols 3 (8 pulses of 1000 $\mu$s at 2500 V cm$^{-1}$) and 4 (80 pulses of 100 $\mu$s at 2500 V cm$^{-1}$) yield complete tumor regression in more than 60% of the cases, thus indicating that tissue

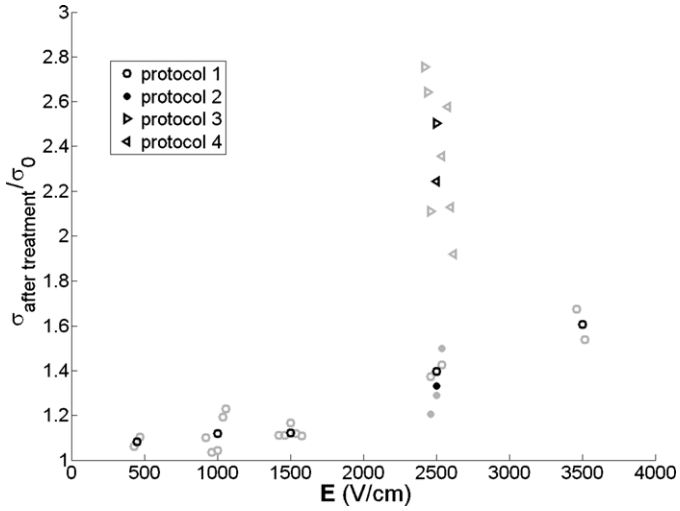


**Figure 5.** Relative conductivity after treatment (50 ms after the end of last pulse) versus field magnitude for different protocols; protocol 1: 8 pulses of 100 $\mu$s at 10 Hz; protocol 2: 8 pulses of 100 $\mu$s at 1 Hz; protocol 3: 8 pulses of 1000 $\mu$s at 0.03 Hz; protocol 4: 80 pulses of 100 $\mu$s at 1 Hz. Black marks indicate the mean values for each protocol and field magnitude. Gray color marks indicate individual experiments. The slight random differences in the field magnitude were artificially introduced for representation purposes.

damage by electroporation was severe. As shown in figure 5, the immediate post-treatment conductivities from protocols 3 and 4 are clearly larger than those from protocol 1, even at 3500 V cm$^{-1}$. This is an indication that the immediate conductivity increase seems to be related to treatment outcome. Moreover, in figure 5, it is also possible to note that the increase in conductance for protocol 1 at fields below 2000 V cm$^{-1}$ is quite constant and moderate in comparison to what it is obtained at 2500 V cm$^{-1}$ and 3500 V cm$^{-1}$ in which, although complete tumor regression is not achieved, some degree of irreversible electroporation is produced.

Note that conductance behavior for protocol 1 has two distinctive patterns: (1) moderate and quite constant at 500 V cm$^{-1}$, 1000 V cm$^{-1}$ and 1500 V cm$^{-1}$ and (2) significantly higher and field dependant, apparently linear, for 2500 V cm$^{-1}$ and 3500 V cm$^{-1}$. This is particularly interesting because the transition region between both behavioral regimes is where we believe that irreversible electroporation is first manifested (from results in Al-Sakere *et al* (2007)). This same observation (i.e. the presence of two distinctive patterns) is also observed in other sort of conductance measurements reported in next sections. We suggest that as long as only reversible electroporation is achieved, changes in conductance remain weak. This observation might be linked to electroporation models in which the formation of large pores, or membrane defects, presumably more stable than small pores and more harmful, manifests a highly nonlinear relationship with the electric field magnitude (Krassowska and Filev 2007).

Figures 3 and 4 clearly indicate that electroporation is a phenomenon that shows memory effects; that is, its behavior will depend on previous pulsing history (Teissie *et al* 2005). Hence, it could be expected that time interval between pulses could have some impact on electroporation effects. On the other hand, Miklavcic *et al* (2005) have demonstrated *in vivo* that the frequency of the pulses is not relevant in terms of electrochemotherapy treatment outcome in the range from 1 Hz to 5 kHz using an electroporation protocol equivalent to our protocol 1 (plus administration of bleomycin). Here we decided to try protocol 2, which

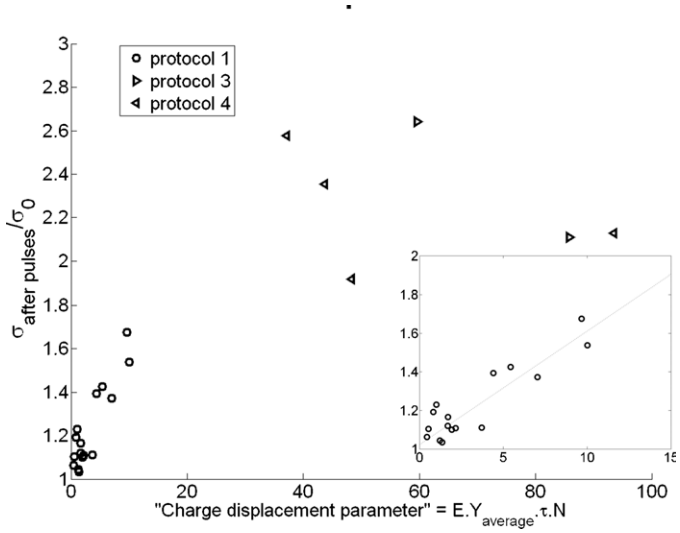


**Figure 6.** Relative conductivity increase after treatment versus applied electric charge during electroporation treatment ('charge displacement parameter' from Grafström *et al* (2006)). $E$ indicates the field magnitude (V cm$^{-1}$), $Y$, is the average admittance value during the electroporation pulses, $\tau$ is the duration of each pulse (100 $\mu$s for protocols 1, 2 and 4 and 1 ms for protocol 3) and $N$ is the number of pulses (8 in protocols 1, 2 and 3 and 80 in protocol 4).

is equivalent to protocol 1 at 2500 V cm$^{-1}$ with a frequency of 1 Hz instead of 10 Hz, to assess whether conductivity changes reflected similarities between both protocols, as it could be expected from Miklavcic *et al*'s results. And our conductivity results indeed show that both frequencies produce similar results (figure 5). Therefore, this fact reinforces previous indications that immediate conductivity changes after treatment can assess outcome

Grafström *et al* (2006) found linear relationships between the applied electric field magnitude and the conductivity increase in rat muscle tissue for fields up to 1800 V cm$^{-1}$. They proposed that the electropermeabilization efficiency (rated by the cellular uptake of extracellular molecules) and conductivity increase are both linearly correlated with the total electric charge injected during electroporation pulses ('$Q$', obtained from current measurement during the pulse). From the experiments performed in the current study, we indeed observe that a linear relationship may exist between the conductivity increase and $Q$ for low $Q$ values (see inset in figure 6) although it seems that such statement is not valid for large $Q$ values (protocols 3 and 4). Nevertheless, it is interesting to note that, in the case of protocol 1, a linear relationship may exist between the conductivity increase and $Q$ whereas the same cannot be said about the relationship between the conductivity increase and the applied field (figure 5).

A practical disadvantage of post-pulse conductivity measurements is that they may be distorted by the electrode–tissue interface impedance if no precautions are taken. In the present study we employed the four-electrode method to avoid such distortion. In cases in which the four-electrode method is not feasible, other two strategies could be tried to avoid, or to minimize, the influence of the electrode–tissue interface impedance: (1) to reduce the interface impedance of the electrodes by increasing their effective area mechanically (e.g. sandblasting) or chemically (e.g. deposition of platinum black (Ivorra and Rubinsky 2007)) and (2) to increase moderately the measurement frequency (e.g. from 1 kHz to 10 kHz).

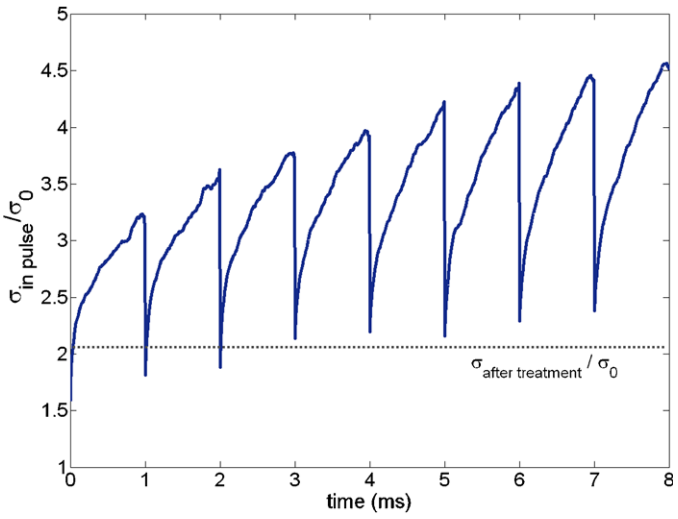


**Figure 7.** Relative in-pulse conductivity (dynamic conductivity) in an experiment from protocol 3 (eight pulses of 1000 $\mu$s at 0.03 Hz). Intervals between pulses (∼33 s) are not displayed.

Electrode–electrolyte interface impedance behaves similarly to a capacitance and therefore its impedance magnitude is higher at lower frequencies. On the other hand, tissue conductance sensitivity to electroporation is higher at lower frequencies. Hence, a trade-off would exist between sensitivity and distortion for choosing the frequency for two-electrode post-pulse conductivity measurements.

### *3.3. 'In-pulse' conductivity*

In-pulse conductivity (equivalent to the term 'dynamic conductivity' employed in nonlinear electronics) was calculated by dividing the current flowing through the electrodes by the voltage applied during the electroporation pulse. Figure 7 shows the evolution of relative in-pulse conductivity for one of the experiments within protocol 3. Note that the in-pulse conductivity increases during each pulse and that it is significantly larger than the conductivity before pulses ($=\sigma_0$) or the conductivity after treatment is completed (in this particular case, $\sigma_{\text{after treatment}}/\sigma_0 \sim 2.1$). Such qualitative features are common to the four protocols at any field magnitude. That is, in all the experiments performed here, the in-pulse conductivity is larger than the conductivity before pulses and larger than the conductivity after treatment.

The step increase in conductivity when each pulse is applied seems to be immediate in terms of the time resolution considered here (1 $\mu$s). Moreover, it is probably masked by the peak in current due to the charging of cell membranes. This is in agreement with previous experimental studies and with models that predict that most pores are immediately ($<1$ $\mu$s) created after the transmembrane voltage overcomes the electroporation threshold (DeBruin and Krassowska 1999). Then, after the voltage drops, it seems that a significant part of the increase in conductivity is also lost in an immediate fashion. Although we do not have data for such voltage drop interval (up to 10 ms after the pulse) the loss of conductivity is not compatible with the slow decay functions we observe afterward (section 3.2). This is also in agreement with previous experimental results (Kinosita *et al* 1988, Hibino *et al* 1993) and would be in agreement with those models that predict the existence of short-lived pores

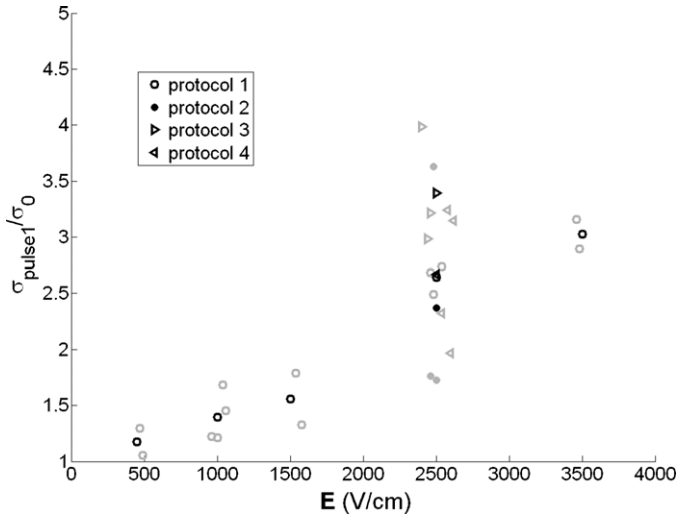


**Figure 8.** Relative average in-pulse conductivity (dynamic conductivity) at the last 10 $\mu$s of the first pulse versus field magnitude for different protocols; protocol 1: 8 pulses of 100 $\mu$s at 10 Hz; protocol 2: 8 pulses of 100 $\mu$s at 1 Hz; protocol 3: 8 pulses of 1000 $\mu$s at 0.03 Hz; protocol 4: 80 pulses of 100 $\mu$s at 1 Hz. Black marks indicate the mean values for each protocol and field magnitude. Gray color marks indicate individual experiments. The slight random differences in the field magnitude were artificially introduced for representation purposes.

(which are created during the pulse and transiently increase conductivity but immediately, in milliseconds, become sealed after high-voltage ceases) and long-lived pores (those would be the ones that we observed in section 3.2 and that contribute to increased permeability for ions and molecules for some seconds or even minutes) (Pavlin *et al* 2005).

Figures 8 and 9 show the average in-pulse conductivity at the last 10 $\mu$s of the pulse relative to the original conductivity (before any pulse has been applied). Figure 8 shows relative conductivity at the end of the first applied pulse and figure 9 shows it at the end of the last applied pulse.

An indication of the quality and repeatability of the measurements is given by the fact that protocols 1, 2 and 4 at 2500 V cm$^{-1}$ produce almost equal results at the end of the first pulse (figure 8).

The fact that conductivity at the end of the pulse is larger than the original conductivity ($\sigma_0$) indicates that some degree of electroporation has occurred in all the cases, even for protocol 1 at 500 V cm$^{-1}$. There is an obvious dependence of the conductivity increase on the electric field magnitude. In the first pulse (figure 8), for protocols 1, 2 and 4, conductivity gradually increases as the electric field magnitude increases. In particular, for field magnitudes 500, 1000 and 1500 V cm$^{-1}$, the dependence seems to be quite linear. The conductivity increase for large field values could also follow another linear dependence but more data points would be needed to hypothesize any sort of function. Nevertheless it is worth noting that, as in the case of post-pulse conductivity, there appears to be some sort of transition in behavior from 1500 V cm$^{-1}$ to 2500 V cm$^{-1}$.

Measurements of the relative conductivity at the last pulse (figure 9) show that previous electroporation pulses had some effect on the conductance of the tissue. This is significantly clearer in protocol 1 at 2500 and 3500 V cm$^{-1}$ and protocols 2, 3 and 4. Up to a point, this is an indication that the last pulse relative conductivity is also correlated with the degree of

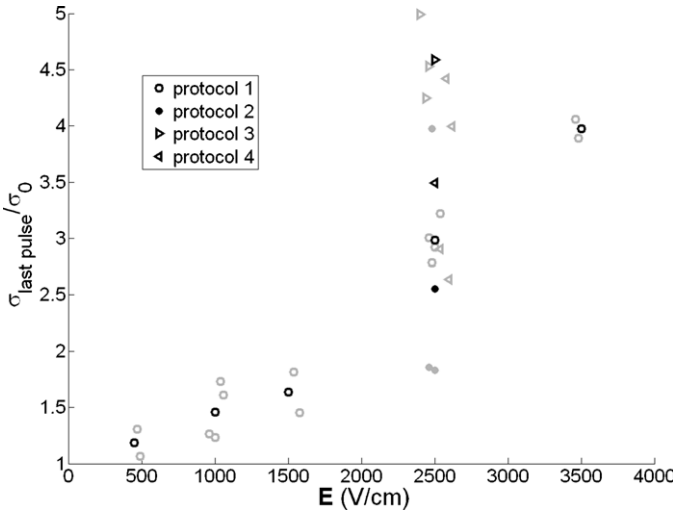


**Figure 9.** Relative average in-pulse conductivity (dynamic conductivity) at the last 10 $\mu$s of the last pulse versus field magnitude for different protocols; protocol 1: 8 pulses of 100 $\mu$s at 10 Hz; protocol 2: 8 pulses of 100 $\mu$s at 1 Hz; protocol 3: 8 pulses of 1000 $\mu$s at 0.03 Hz; protocol 4: 80 pulses of 100 $\mu$s at 1 Hz. Black marks indicate the mean values for each protocol and field magnitude. Gray color marks indicate individual experiments. The slight random differences in the field magnitude were artificially introduced for representation purposes.

damage caused by irreversible electroporation. However, it must be mentioned that although protocol 1 at 3500 V cm$^{-1}$ produces higher last-pulse conductivity than protocol 4 we know from the study reported in Al-Sakere *et al* (2007) that tissue damage induced by protocol 4 is much more severe. Hence last-pulse conductivity does not seem to be such a good prognostic indicator as immediate post-treatment conductivity.

It is worth noting that the maximum in-pulse relative conductivity is about 5 (figure 9). This implies an in-pulse conductivity of about 6 mS cm$^{-1}$ which is similar to the maximum conductivity we observed in muscle electroporation experiments at 1500 V cm$^{-1}$ (Ivorra *et al* 2007). We hypothesize that in both cases the membrane impedance has become irrelevant. That is, membrane has become so permeable to ions that its resistance is insignificant when compared to the resistance of the intracellular and the extracellular media. Such statement does not imply that the membrane is completely disrupted; only a tiny fraction of the membrane needs to be disrupted in order to achieve such irrelevance in terms of conductivity (Hibino *et al* 1993).

### *3.4. Long-term conductivity evolution after treatment*

In all experiments, impedance was measured for 30 min after electroporation treatment. After the initial drop in conductivity compatible with logarithm evolution described in section 3.2, relative conductivity decreases at a lower rate toward the pre-treatment value $\sigma_0$ (figure 10). In some cases (protocol 1 at 500, 1000 and 1500 V cm$^{-1}$), it even gets to values lower than the original conductivity value. This phenomenon also happened in the livers subjected to reversible electroporation and, to some extent, in those subjected to irreversible electroporation. It is probably a clear indication of membrane resealing combined with, or followed by, cellular edema due to unbalanced osmotic pressure (Abidor *et al* 1994) (see Ivorra and Rubinsky (2007) for other possible explanations).

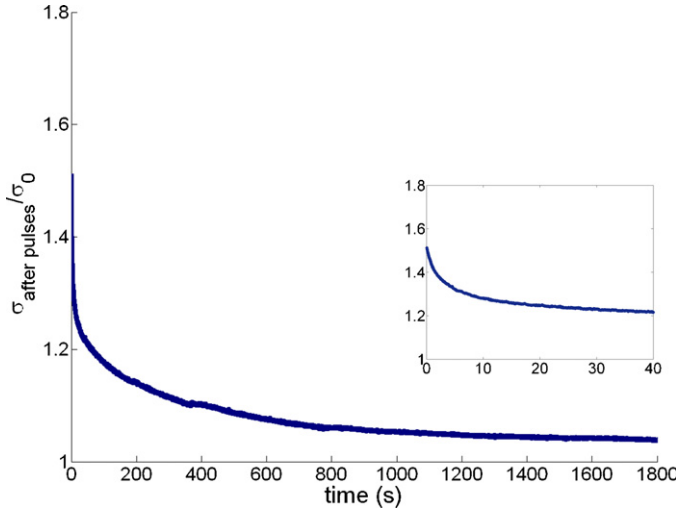


**Figure 10.** Conductivity evolution after treatment from an experiment belonging to protocol 1 (eight pulses of 100 $\mu$s at 10 Hz) at 2500 V cm$^{-1}$. The inset is a magnification of the first 40 s.

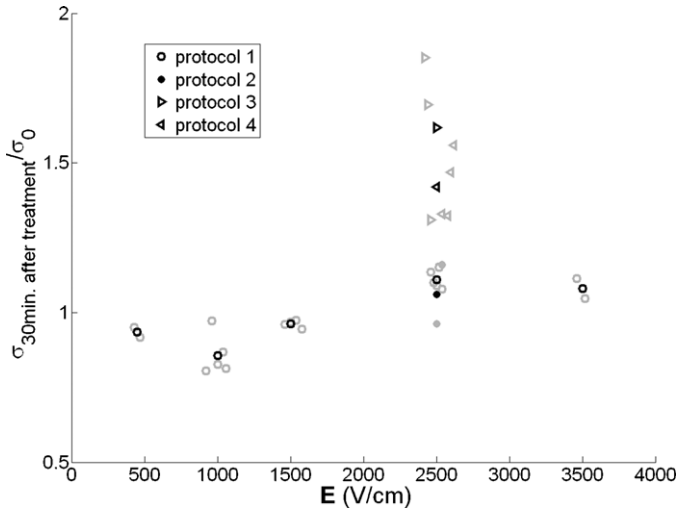


**Figure 11.** Relative conductivity 30 min after treatment versus field magnitude for different protocols; protocol 1: 8 pulses of 100 $\mu$s at 10 Hz; protocol 2: 8 pulses of 100 $\mu$s at 1 Hz; protocol 3: 8 pulses of 1000 $\mu$s at 0.03 Hz; protocol 4: 80 pulses of 100 $\mu$s at 1 Hz. Black marks indicate the mean values for each protocol and field magnitude. Gray color marks indicate individual experiments. The slight random differences in the field magnitude were artificially introduced for representation purposes.

However, compared with liver behavior here the decrease toward pre-pulse values seems much slower. Another significant difference, the sudden drop of resistivity that occurred at about 15 min after IRE in liver, here is not manifested. We attributed that decrease to sudden cell rupture, or cell fusion, triggered somehow by electroporation.

Figure 11 shows relative conductivity values 30 min after treatment. Note that samples subjected to protocol 1 at low fields (500, 1000 and 1500 V cm$^{-1}$) recover their original conductivity ($\sigma_{30\text{ min after treatment}} = \sigma_0$) and that some cases show lower conductivities. On the

other hand, samples subjected to larger fields or to protocols 2, 3 and 4 do not reach their original conductivity. At 2500 V $cm^{-1}$, samples from protocols 3 and 4 show conductivity values clearly larger than those of samples from protocols 1 and 2. Hence 'long-term' conductivity is probably a good indicator for damage by irreversible electroporation.

## 4. Conclusions

Probably the most significant conclusion that can be drawn from the study presented here is the fact that post-treatment conductivity indeed seems to be correlated with treatment outcome in terms of reversibility. This would be valid for immediate conductivity assessment after the pulse sequence and for measurements taken 30 min thereafter.

Conductivity measurements taken from voltage and current measurements during the application of the last electroporation pulse also seem to show some degree of correlation with tissue damage. However, in this case the distinction between some experimental protocols is not so clear as for the case of post-treatment measurements.

An interesting observation is that pulse repetition slows down conductivity decay after the pulse. This probably indicates that permeabilization becomes more stable due to multiple pulses.

## Acknowledgments

This work was supported by grants of the CNRS and the IGR, by the French National Agency (ANR) through the Nanoscience and Nanotechnology Program (Nanopulsebiochip ANR-08-NANO-024) and by the US National Institutes of Health (NIH) under grant NIH R01 RR018961. The staff of the Service Commun d'Expérimentation Animale (headed by Dr P Gonin) is also acknowledged for mice housing. BR has a financial interest in Excellin Life Sciences and Oncobionic which are companies in the field of electrical impedance tomography of electroporation and irreversible electroporation, respectively.

## References

Abidor I G, Li L H and Hui S W 1994 Studies of cell pellets: II. Osmotic properties electroporation and related phenomena: membrane interactions *Biophys. J.* **67** 427–35

Al-Sakere B, André F, Bernat C, Connault E, Opolon P, Davalos R V, Rubinsky B and Mir L M 2007 Tumor ablation with irreversible electroporation *PLoS ONE* **2** e1135

Belehradek J, Barski G and Thonier M 1972 Evolution of cell-mediated antitumor immunity in mice bearing a syngeneic chemically induced tumor. Influence of tumor growth surgical removal and treatment with irradiated tumor cells *Int. J. Cancer* **9** 461–9

Cegovnik U and Novaković S 2004 Setting optimal parameters for *in vitro* electrotransfection of B16F1 SA1 LPB SCK L929 and CHO cells using predefined exponentially decaying electric pulses *Bioelectrochemistry* **62** 73–82

Cima L F and Mir L M 2004 Macroscopic characterization of cell electroporation in biological tissue based on electrical measurements *Appl. Phys. Lett.* **85** 4520–22

Cukjati D, Batiuskaite D, Andre F, Miklavcic D and Mir L M 2007 Real time electroporation control for accurate and safe *in vivo* non-viral gene therapy *Bioelectrochemistry* **70** 501–7

Davalos R V, Mir L M and Rubinsky B 2005 Tissue ablation with irreversible electroporation *Ann. Biomed. Eng.* **33** 223–31

Davalos R V, Rubinsky B and Otten D M 2002 A feasibility study for electrical impedance tomography as a means to monitor tissue electroporation for molecular medicine *IEEE Trans. Bio-Med. Eng.* **49** 400–3

Dean D A 2005 Nonviral gene transfer to skeletal smooth and cardiac muscle in living animals *Am. J. Physiol. Cell Physiol.* **289** C233–45

DeBruin K A and Krassowska W 1999 Modeling electroporation in a single cell: I. Effects of field strength and rest potential *Biophys. J.* **77** 1213–24

Dev S B, Dhar D and Krassowska W 2003 Electric field of a six-needle array electrode used in drug and DNA delivery *in vivo*: analytical versus numerical solution *IEEE Trans. Bio-Med. Eng.* **50** 1296–300

Edd J, Horowitz L, Davalos R V, Mir L M and Rubinsky B 2006 *In vivo* results of a new focal tissue ablation technique: irreversible electroporation *IEEE Trans. Bio-Med. Eng.* **53** 1409–15

Ghosh P M, Keese C R and Giaever I 1993 Monitoring electropermeabilization in the plasma membrane of adherent mammalian cells *Biophys. J.* **64** 1602–9

Glahder J, Norrild B, Persson M B and Persson B R 2005 Transfection of HeLa-cells with pEGFP plasmid by impedance power-assisted electroporation *Biotechnol. Bioeng.* **92** 267–76

Gothelf A, Mir L M and Gehl J 2003 Electrochemotherapy: results of cancer treatment using enhanced delivery of bleomycin by electroporation *Cancer Treat. Rev.* **29** 371–87

Grafström G, Engström P, Salford L G and Persson B R 2006 $^{99m}$Tc-DTPA uptake and electrical impedance measurements in verification of *in vivo* electropermeabilization efficiency in rat muscle *Cancer Biother. Radiopharm.* **21** 623–35

Hibino M, Itoh H and Kinosita K 1993 Time courses of cell electroporation as revealed by submicrosecond imaging of transmembrane potential *Biophys. J.* **64** 1789–800

Huang Y and Rubinsky B 1999 Micro-electroporation: improving the efficiency and understanding of electrical permeabilization of cells *Biomed. Microdevices* **2** 145–50

Ivorra A, Miller L and Rubinsky B 2007 Electrical impedance measurements during electroporation of rat liver and muscle *IFMBE Proc. of the 13th Int. Conf. on Electrical Bioimpedance and the 8th Conf. on Electrical Impedance Tomography* vol 17 pp 130–3

Ivorra A and Rubinsky B 2007 In vivo electrical impedance measurements during and after electroporation of rat liver *Bioelectrochemistry* **70** 287–95

Jaroszeski M J, Heller R and Gilbert R 2000 *Electrochemotherapy Electrogenetherapy and Transdermal Drug Delivery* (Totowa, NJ: Humana Press)

Jossinet J and Schmitt M 1999 A review of parameters for the bioelectrical characterization of breast tissue *Ann. New York Acad. Sci.* **873** 30–41

Kinosita K J, Ashikawa I, Saita N, Yoshimura H, Itoh H, Nagayama K and Ikegami A 1988 Electroporation of cell membrane visualized under a pulsed-laser fluorescence microscope *Biophys. J.* **53** 1015–9

Kinosita K J and Tsong T Y 1979 Voltage-induced conductance in human erythrocyte membranes *Biochim. Biophys. Acta* **554** 479–97

Krassowska W and Filev P D 2007 Modeling electroporation in a single cell *Biophys. J.* **92** 404–17

Miklavcic D *et al* 2005 The effect of high frequency electric pulses on muscle contractions and antitumor efficiency *in vivo* for a potential use in clinical electrochemotherapy *Bioelectrochemistry* **65** 121–8

Miller L, Leor J and Rubinsky B 2005 Cancer cells ablation with irreversible electroporation *Technol. Cancer Res. Treat.* **4** 699–705

Mir L M 2001 Therapeutic perspectives of *in vivo* cell electropermeabilization *Bioelectrochemistry* **53** 1–10

Neumann E, Schaeffer-Ridder M, Wang Y and Hofschneider P H 1982 Gene transfer into mouse lyoma cells by electroporation in high electric fields *EMBO J.* **1** 841–5

Pavlin M, Kanduser M, Rebersek M, Pucihar G, Hart F X, Magjarevic R and Miklavcic D 2005 Effect of cell electroporation on the conductivity of a cell suspension *Biophys. J.* **88** 4378–90

Pavlin M and Miklavcic D 2008 Theoretical and experimental analysis of conductivity ion diffusion and molecular transport during cell electroporation—relation between short-lived and long-lived pores *Bioelectrochemistry* **74** 38–46

Pliquett U, Elez R, Piiper A and Neumann E 2004 Electroporation of subcutaneous mouse tumors by rectangular and trapezium high voltage pulses *Bioelectrochemistry* **62** 83–93

Prozorov R and Prozorov T 2004 Effective collective barrier for magnetic relaxation in frozen ferrofluids *J. Magn. Magn. Mater.* **281** 312–7

Pucihar G, Kotnik T, Kanduser M and Miklavcic D 2001 The influence of medium conductivity on electropermeabilization and survival of cells *in vitro Bioelectrochemistry* **54** 107–15

Rubinsky B, Onik G and Mikus P 2007 Irreversible electroporation: a new ablation modality—clinical implications *Technol. Cancer Res. Treat.* **6** 37–48

Stämpfli R 1957 Reversible electrical breakdown of the excitable membrane of a Ranvier node *An. da Acad. Bras. de Cienc.* **30** 57–63

Teissie J, Golzio M and Rols M P 2005 Mechanisms of cell membrane electropermeabilization: a minireview of our present (lack of ?) knowledge *Biochim. et Biophys. Acta* **1724** 270–80

United Kingdom Co-ordinating Committee on Cancer Research (UKCCCR) 1998 Guidelines for the welfare of animals in experimental neoplasia (2nd edition) *Br. J. Cancer* **77** 1–10